EAXL: Electrodeposition Assisted X-ray Lithography

John P. Katsoudas[1]*

Elena V. Timofeeva[2]

Carlo U. Segre[1]

[1] Physics Department & Center for Synchrotron Radiation Research and Instrumentation, Illinois Institute of Technology, Chicago, IL 60616, USA

[2] Energy Systems Division, Argonne National Laboratory, Argonne, IL 60439, USA

*e-mail: katsjoh@iit.edu

APRIL 2011

The submitted manuscript has been created by Argonne National Laboratory, a U.S. Department of Energy laboratory managed by UChicago Argonne, LLC, under Contract No. DE-AC02-06CH11357 with the U.S. Department of Energy. The U.S. Government retains for itself, and others acting on its behalf, a paid-up, nonexclusive, irrevocable worldwide license in said article to reproduce, prepare derivative works, distribute copies to the public, and perform publicly and display publicly, by or on behalf of the Government

To be submitted to ELECTROCHEMICAL AND SOLID STATE LETTERS

EAXL: Electrodeposition Assisted X-ray Lithography

John P. Katsoudas[1]*, Elena V. Timofeeva[2], Carlo U. Segre[1]

[1] Physics Department & Center for Synchrotron Radiation Research and Instrumentation, Illinois Institute of Technology, Chicago, IL 60616, USA

[2] Energy Systems Division, Argonne National Laboratory, Argonne, IL 60439, USA

*e-mail: katsjoh@iit.edu

This paper reports on the development of a novel single-step approach for the formation of patterned metal deposits from metal salt solution using an x-ray lithography technique. Electrodeposition assisted X-ray lithography (EAXL) is based on simultaneously exposing the substrate to masked x-rays within an electric field, utilizing radiolysis and potentiostatic electrodeposition. The EAXL results demonstrate patterned silver deposition from the salt solution without the use of resist-substrate material and confirm that simultaneous exposure to x-rays with the application of an electric filed was required in obtaining the patterned metal deposits. The results are promising for MEMS and NEMS manufacturing and also demonstrate the fundamental phenomena of synergetic effect of x-rays and electric field.

Introduction

The microelectromechanical systems (MEMS) can have high aspect ratios with dimensions that often exceed the limits of traditional fabrication methods. As technologies incorporate the nanoscale (NEMS) this limitation will continue to grow. The resolutions of extreme ultraviolet and visible light lithography have diffraction and beam focusing limitations. An x-ray wavelength is on the order of the atomic scale thus providing few limitations related to their resolving power. LIGA (x-ray lithography, or *Lithographie, Galvanoformung,* and *Abformung*) has been recognized and developed as a unique technique that provides high precision, spatial resolution, and high aspect ratio [1]. In a typical LIGA process, a thick photo resist (PMMA or

EPON SU-8) is exposed to a masked x-ray beam (deep x-ray lithography or DXRL step). The developed-processed resist is then used as an electroplating template. After overplating, a mold is stripped from the polymer substrate, and employed in a mass production scheme such as injection molding or hot embossing. Despite all the technical advantages LIGA is still a niche technology with a rather limited spectrum of commercial applications. The major drawbacks to LIGA are cost and slow production rates.

Being a multistep, sequential process, LIGA relies on many process variables, and its ability to produce consistently acceptable structures is proportional to the amount of time and effort invested in each of the manufacturing steps. The physical exposure time for DXRL structures typically run between 4 and 8 hours (PMMA) of synchrotron beam time, which is an extremely expensive proposition from a "cost of exposure time vs. production" point of view.

Minimization of as many processing steps as possible would make the x-ray lithography process a much more efficient and cost effective manufacturing technique. Therefore the traditional template molding and electroplating steps were targeted for elimination in our proof of concept experiment. The novel method that is presented in this work forgoes 4 of the traditional processing steps involved in fabricating high aspect ratio metallic structures, providing the proof of principle for single step patterning with x-ray lithography.

Synchrotron radiation was used because of its advantageous ability to penetrate the metal salt solution within the experimental cell, while maintaining a high degree of collimation, and the availability of a wide (~10 cm) beam from a bending magnet source. Any other exposure source (ultraviolet or soft x-ray) would either dissipate before patterning occurred, or could not be masked (γ-ray) within the regimes of DXRL.

Experimental

The experimental cell (Fig. 1) consisted of two graphite plates that served as x-ray bulkhead windows and as the working and counter electrodes sandwiched between three Teflon plates. A silver-silver chloride (Ag/AgCl) electrode was used as a reference electrode. An electrolyte

solution (0.1 M $AgNO_3$ in DI water) was circulated in a closed loop by a peristaltic pump at flow rates 100-300 ml/min. Electrodeposition was conducted in a potentiostatic regime at low overpotentials (150 mV negative of Nernst equilibrium potential, or 0.35 V vs. Ag/AgCl) in order to provide homogeneous growth of the deposits.

The lithography mask was attached to the upstream face of the cell, and the entire assembly was vertically scanned through the incident x-ray beam (size vert. 2 mm x hor. 62 mm) using an Aerotech UNIDEX 500 lithography scanner (machine resolution .0001 mm). The 879.50 mm long Pt coated mirror of beam line 10-BM-A at the Advanced Photon Source was employed as a low bandpass filter whose cutoff energy was determined by the angle between the incident beam and mirror. The mirror angle was set to 2.25 mRad, which was calculated to produce an energy spectrum with an x-ray absorption length of approximately one cell thickness (2.5 cm) and accounted for all optically active components of the cell.

Results and Discussion

Irradiation of aqueous solution of metal ions leads to the radiolysis of water resulting in the formation of radicals, among which solvated electrons (e^-_{aq}) are strong reducing agents for the metal ions [2]. Their induced reduction leads to the formation of atoms, which aggregate and form metallic clusters. This technique has been successfully used in micro- and nano- fabrication either with a γ-ray source [3-4], laser or electron beam [5] or more recently with x-rays [6-8]. Our EAXL approach to form a metallic object of controlled size and shape relies on the superposition of the radiolytic reduction of metal ions into atoms with the controlled potentiostatic deposition from metal salt solution. No pattern was formed on the substrate during the exposure to masked x-rays at open cell circuit. The electrodeposition potential is maintained at the value where the deposition rate is just slightly higher than the metal dissolution rate. The electrodeposition process promotes nucleation and growth of crystals under the influence of an electric field. Competition between growth and nucleation determines the granularity, structure and properties of the metallic deposits [9]. The hypothesis tested in our series of experiments is

that simultaneous exposure to the masked x-ray beam and a low electrochemical overpotential induces patterned nucleation sites at the electrode through the radiolysis mechanism [6] while the electrochemically controlled growth of those nuclei produces a patterned metal deposit. This technique allows metal deposition only in the areas exposed to patterned x-rays, while minimizing the random nucleation outside the exposed areas.

Figure 2 illustrates the results of simultaneous exposure of graphite electrode in 0.1 M $AgNO_3$ solution. Continuous shapes of interconnected metal crystallites (Fig. 2b) formed in the areas where the mask (Fig. 2a) allowed penetration of x-rays. The pattern is composed of nearly spherical single crystal grains 10-40 μm in diameter. The width of the deposit is very close to the feature size of the mask. The deviations from the pattern (±10 μm or ~20%) observed and are most likely due to the non-selective 3D growth of sites nucleated within the x-ray pattern.

The topography of the deposits has been reconstructed using z-stack extended focus optical 3D imaging (Fig. 3a). The image profile shows (Fig. 3b) that the deposits have an approximate aspect ratio of ~ 1:1 confirming the non-selective growth of nucleated sites. The roughness of the initial surface was quite high, indicating a wide range of surface energies - a potential obstacle towards obtaining homogeneous nucleation. To improve the quality and aspect ratio of the pattern the use of a more homogeneous electrode substrate and/or creating conditions for a selective growth in one crystal plane is suggested.

Conclusions

In this paper we demonstrated the formation of a patterned silver deposit from salt solution on porous graphite plates without the use of any resist-substrate material. The superposition of masked x-rays and an electric field was used to obtain the patterns. The silver deposits are polycrystalline continuous structures with less than 20% deviation from the mask features. Due to a non-selective growth of nucleation centers formed in the x-ray path the current aspect ratio is nearly 1:1, but could be significantly improved by using a more homogeneous electrode surface and controlling the selective growth in one crystal plane. Further work in this direction will

allow this technique to establish itself as a candidate for future micro- and nanomanufacturing development. Besides the results clearly demonstrate the synergetic effect of x-rays and electric field that should be accounted for when electrochemical systems are characterized with x-ray techniques.

Acknowledgements

We thank Ralu Divan for her guidance and help, Jeremy Kropf for his critical opinion on design and the concept of the experiments, and NuVant Inc. for providing us with equipment for electrochemical part of the experiment. Many thanks to Nicholas Andrisevic and Brad Etter from Carl Zeiss Inc. for help with 3D topography of the samples. MRCAT operations are supported by the Department of Energy and the MRCAT member institutions. Use of the Advanced Photon Source is supported by the U.S. Department of Energy, Office of Science, Office of Basic Energy Sciences, under Contract No. DE-AC02-06CH11357.

References

(1) V. Saile, U. Wallrabe, O. Tabata, J.G. Korvink, Eds., *LIGA and Its Applications*, Vol. 7., Wiley-VCH: Weinheim, Germany (2009).

(2) G.V. Buxton, R.M. Sellers, *Coordination Chemistry Reviews*, **22**, 195 (1977).

(3) D.B. Yu, X.Q. Sun, J.T. Bian, Z.C. Tong, Y.T. Qian, *Physica E-Low-Dimensional Systems & Nanostructures*, **23**, 50 (2004).

(4) H. Remita, I. Lampre, M. Mostafavi, E. Balanzat, S. Bouffard, *Radiation Physics and Chemistry,* **72**, 575 (2005).

(5) F. Stellacci, C.A. Bauer, T. Meyer-Friedrichsen, W. Wenseleers, V. Alain, S.M. Kuebler, S. J. K. Pond, Y. D. Zhang, S. R.Marder, J. W. Perry, *Advanced Materials*, **14**, 194 (2002).

(6) R. Divan, D.C. Mancini, N. Moldovan, L. Assoufid, Y.S. Chu, Q. Ma, R.A. Rosenberg, *2003 International Semiconductor Conference,* Proceedings Vols 1 and 2, p. 39, (2003).

(7) Q. Ma, R. Divan, D.C. Mancini, R.A. Rosenberg, J.P. Quintana, D.T. Keane, *Applied Physics Letters*, **89**, 83114 (2006).

(8) M.F. Bertino, R.R. Gadipalli, L.A. Martin, L.E. Rich, A.Yamilov, B.R. Heckman, N. Leventis, S. Guha, J. Katsoudas, R. Divan, D.C. Mancini, *Nanotechnology*, **18**, 315603 (2007).

(9) E. Budevski, G. Staikov, W.J. Lorenz, *Electrochemical Phase Formation and Growth. An introduction to the Initial Stages of Metal Deposition*, VCH Verlagsgesellschaft mbH: Weinheim, Germany (1996).

Figure Captions:

Figure 1. Experimental cell for simultaneous exposure to X-rays and electric field: R.E. – Ag/AgCl reference; W.E. – working; C.E. – counter electrode.

Figure 2. Optical microscopy images of (a) the lithography mask – inverse pattern of gold deposited onto the silicon wafer; (b) silver pattern formed on the graphite electrode.

Figure 3. (a) 3D topographical image of Ag deposit and (b) estimation of the aspect ratio from the profile.

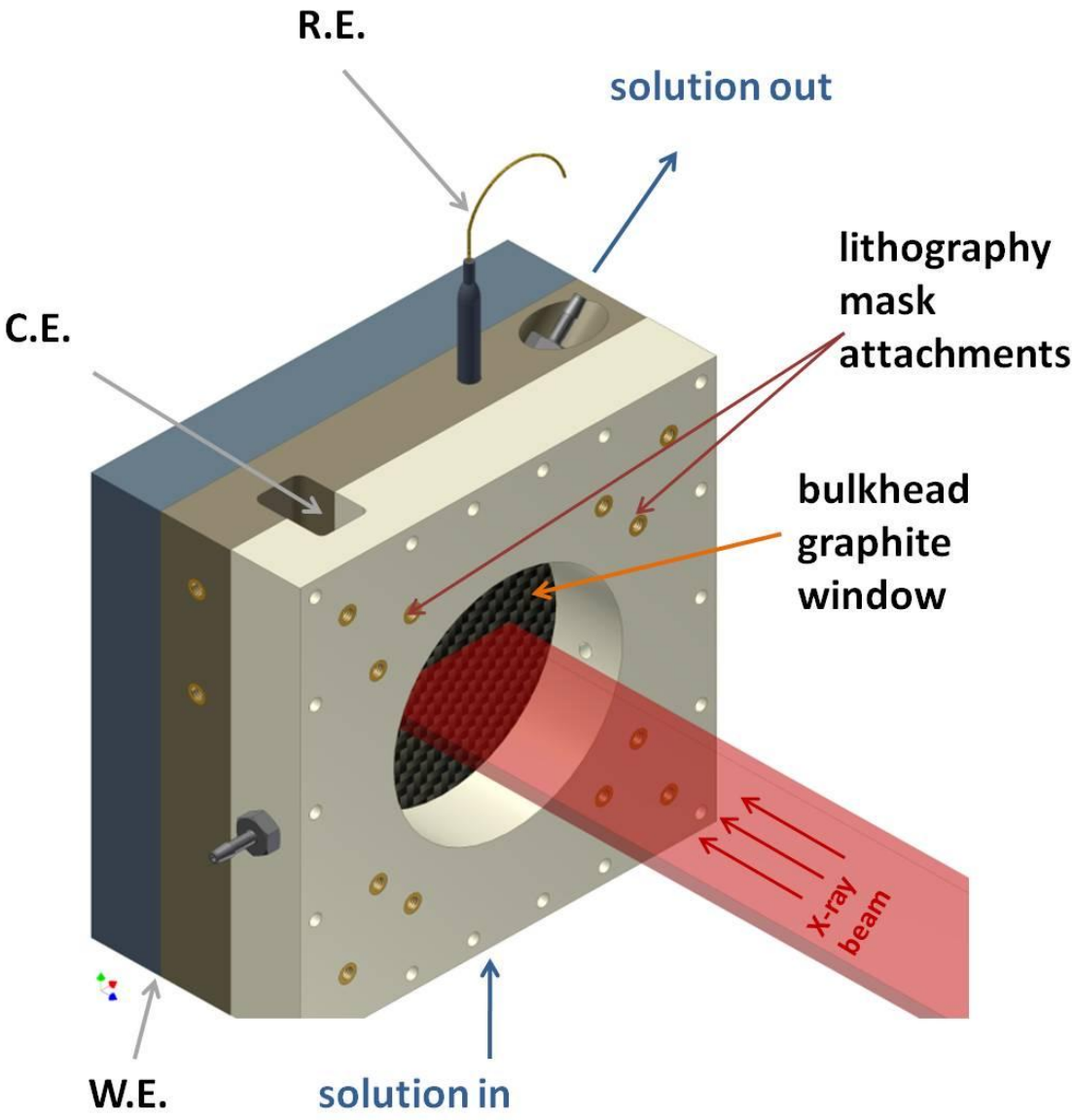
R.E.
solution out
lithography
mask
attachments
C.E.
bulkhead
graphite
window
X-ray
beam
W.E.
solution in

Figure 1.

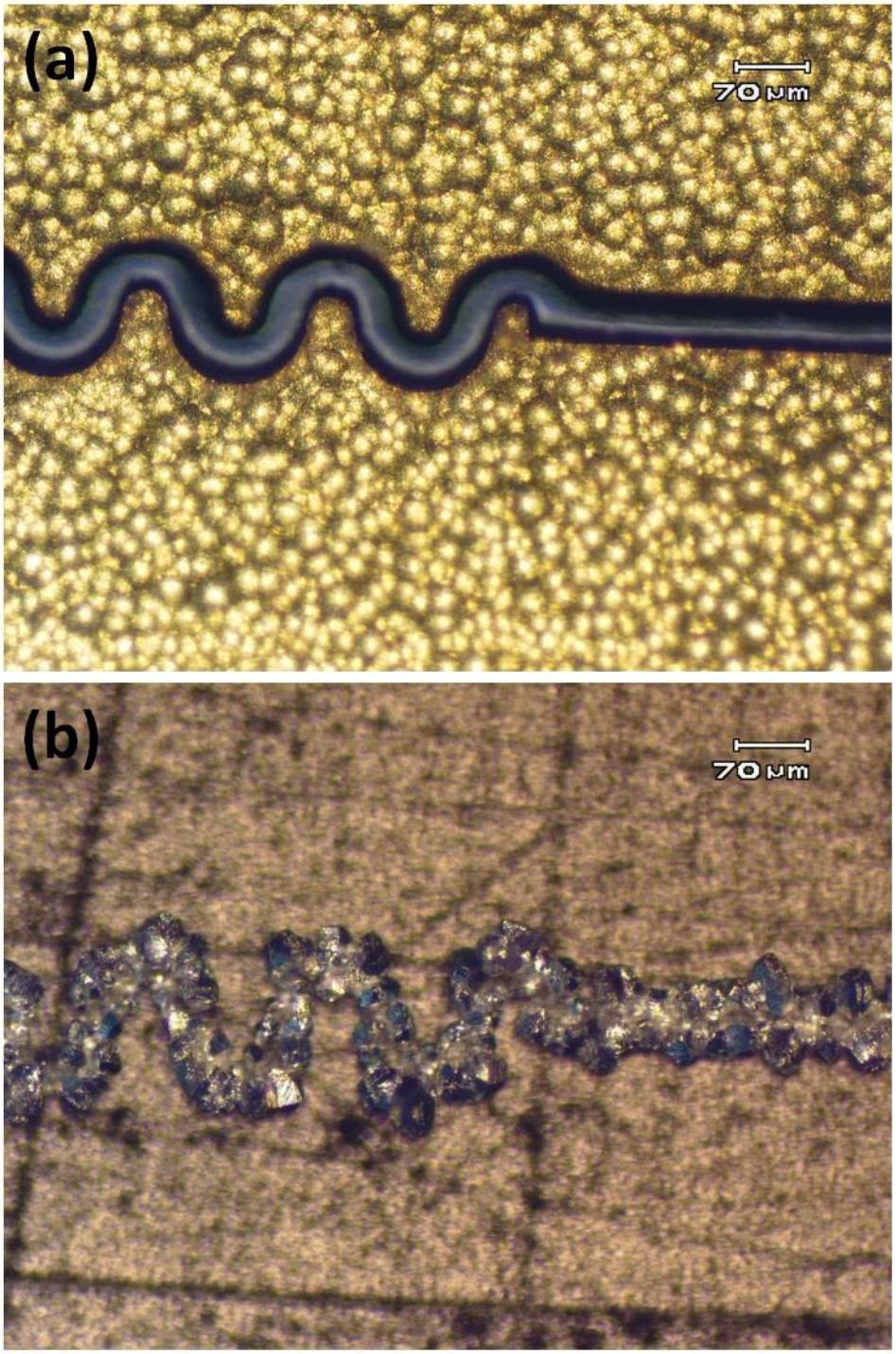

Figure 2.

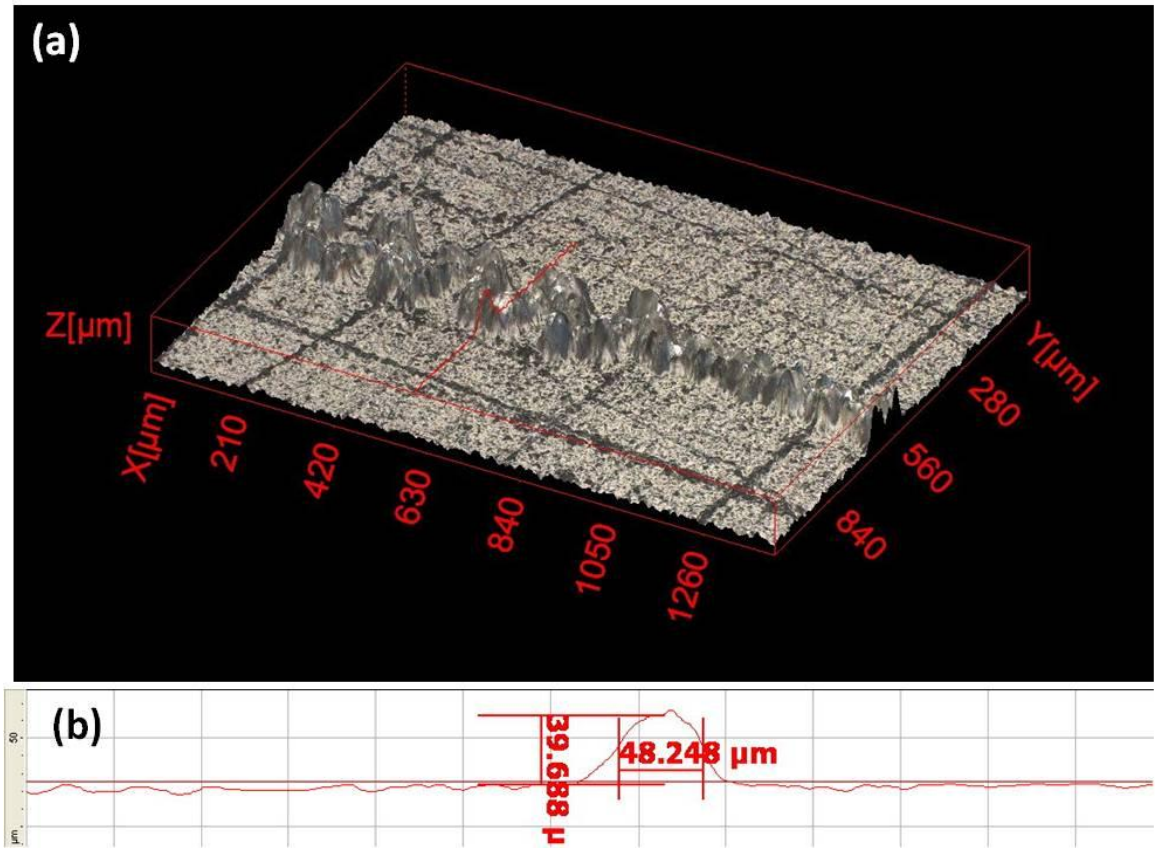
(a)
Z[µm]
X[µm]
210
420
630
840
1050
1260
Y[µm]
280
560
840
(b)
39.688 µm
48.248 µm

Figure 2.